Article

The Plant Specific Insert as an Unconventional Signal in the Route to Plant Vacuoles

Vanessa Vieira[1*], Bruno Peixoto[1,2*], Mónica Costa[1], Susana Pereira[1,3], José Pissarra[1,3], Cláudia Pereira[1,3†]

[1] Faculdade de Ciências da Universidade do Porto. Rua do Campo Alegre, s/nº, 4169 007, Porto, Portugal.
[2] Instituto Gulbenkian de Ciência; Rua da Quinta Grande 6, 2780-156 Oeiras, Portugal (actual address)
[3] GreenUPorto - Sustainable Agrifood Production Research Center. Campus de Vairão, Rua Padre Armando Quintas 7, 4485-661 Vila do Conde, Portugal.
* These authors contributed equally to this work.
† Correspondence: cpereira@fc.up.pt

Abstract: In plant cells the conventional route to the vacuole involves the endoplasmic reticulum, the Golgi and the prevacuolar compartment. However, over the years, unconventional sorting to the vacuole, bypassing the Golgi, has been described, which is the case of the Plant Specific Insert (PSI) of the aspartic proteinase cardosin A. Interestingly, this Golgi-bypass ability is not a characteristic shared by all PSIs, since two related PSIs showed to have different sensitivity to ER-to-Golgi blockage. Given the high sequence similarity between the PSIs domains, we sought to depict the differences in terms of post-translational modifications. In fact, one feature that draws our attention is that one is N-glycosylated and the other one is not. Using site-directed mutagenesis to obtain mutated versions of the two PSIs, with and without the glycosylation motif, we observed that altering the glycosylation pattern interferes with the trafficking of the protein as the non-glycosylated PSI-B, unlike its native glycosylated form, is able to bypass ER-to-Golgi blockage and accumulate in the vacuole. This is also true when the PSI domain is analyzed in the context of the full-length cardosin. Regardless of opening exciting research gaps, the results obtained so far need a more comprehensive study of the mechanisms behind this unconventional direct sorting to the vacuole.

Keywords: Plant Specific Insert, Aspartic Proteinase, Vacuolar Sorting, unconventional trafficking, Endoplasmic Reticulum, Golgi, N-linked glycosylation

1. Introduction

In the last years, the outburst of data on molecular mechanisms involved in endocytic and exocytic trafficking have outlined subtle balances between these pathways. The study of specific cases indicates that membrane and cargo molecules exchange within the cells or in response to the external cell environment is finely tuned [1–3]. In higher plants, the presence of two types of vacuoles, sometimes co-existing, necessarily implies the existence of different sorting mechanisms for each one of these organelles [4–6]. The recognition of these vacuolar sorting determinants (VSDs) generally occurs at the late or post-Golgi level [5, 6], redirecting the protein away from the secretory pathway, and towards the vacuole. Parallel to the conventional Endoplasmic Reticulum (ER) > Golgi > prevacuolar compartment (PVC) route to the vacuole, a more unconventional sorting to the vacuole that bypasses the Golgi has been described in recent years [7–11]. Often, the relevance of this sorting mechanism depends on the type of tissue/cell they are expressed in and the metabolic activity of such organs. This is the case of cardosin A's – an aspartic proteinase from *Cynara cardunculus* - PSI driven transport [8]. A poly-sorting mechanism for cardosin A, with two different vacuolar signals: the C-terminal peptide, a Ct-VSD by definition and the PSI, a more unconventional sorting determinant, is

also discussed by the authors. It was demonstrated that each domain determines a different route to the vacuole in *N. tabacum* leaves: the PSI is able to bypass the Golgi, while the C-terminal peptide follows a classic ER-Golgi-PVC route to the vacuole. This poly-sorting mechanism seems to be related to the different roles of the protein *in planta* and associated with specific cell needs [8, 12].

A wide range of vacuolar plant aspartic proteinases (APs; EC 3.4.23) have been described in a series of different plant species and tissues. Some of these plant enzymes possess an internal segment of approximately 100 amino acids, called Plant Specific Insert (PSI), localized between the enzyme's N- and C-terminal regions [13]. Often absent from the mature AP, this domain regularly shows higher plasticity, both in terms of cDNA and amino-acid sequences. The PSI domain of some aspartic proteinases has been extensively studied given its ability to interact with lipids from the membranes and promote the release of vesicle content *in vitro* [14, 15]. All these particular features have raised the interest in this domain and several studies were conducted using PSIs isolated from different plant species in an attempt to better characterize this domain, considered to be "an enzyme inside an enzyme" [16–20]. Though its functions *in planta* are still highly debated, some reports have been made, where this domain was responsible for AP vacuolar targeting [8, 14, 19, 21]. In fact, Pereira and co-workers (2013) showed that the PSIs from two different cardosins (APs isolated from *Cynara cardunculus*) are able to redirect secreted proteins to the vacuole and that different PSI domains may follow different routes to the lytic vacuole of *Nicotiana tabacum* by a process not yet clearly understood [8]. A working model for cardosins trafficking suggests that the PSI mediates either a COPII-independent or COPII-dependent pathway depending on its glycosylation status, as cardosin A PSI, contrary to cardosin B, is not glycosylated.

To understand both the roles and significance of these two PSI domains in vacuolar targeting, we isolated the PSIs and generated glycosylation mutants for analysis by transient expression in *Nicotiana tabacum* leaf epidermis. Furthermore, we wanted to test if the differences observed with the isolated PSIs would persist when they are expressed in the full-length cardosin. To achieve that we produced different constructs regarding the full length cardosin A and B: two with the native PSI domain and two with swapped PSI domains. The results obtained indicate that cardosin A PSI ability to bypass the Golgi is maintained in the context of the full-length protein and also that glycosylation seems to have a preponderant role in this process. As a proof of concept, we finally isolated two PSIs from *Glycine max* aspartic proteinases, showing the same glycosylation dichotomy, and the results obtained are in agreement to the role of glycosylation we propose. Overall, we expect to have a better definition on how the PSI ER-to-Vacuole direct sorting is orchestrated, through which mechanism this is occurring, and to define the intermediate players in the process.

2. Results

2.1. Different PSIs translate into different sorting routes to the vacuole

Our lab has previously shown that cardosin A has two different vacuolar sorting domains: the PSI and the C-terminal peptide [8]. Upon isolation of the two domains, it was also disclosed that they follow different routes to the vacuole, with the PSI taking a shortcut driving a Golgi-independent pathway. The question raised was if all the PSIs have this ability. Cardosin B is another well-studied aspartic proteinase from cardoon, with a similar structure and high similarity in terms of protein sequence (Figure 1A). We isolated the PSI from cardosin B and placed it between the signal peptide (SP) from *A. thaliana* chitinase and mCherry (Figure 2B). We co-expressed both PSIs in *N. tabacum* leaf epidermis with the ER marker GFP::HDEL [22] and the Golgi marker ST::GFP [23]. It is clear that, 3 days post-infiltration (dpi) PSI-A and PSI-B mCherry fusions are accumulated in the vacuole (Figure 1C) and fluorescence is detected in the ER or Golgi. Both PSI-A and PSI-B are sufficient and efficient in directing mCherry to the vacuole. Next, we sought to depict their route to the vacuole using the dominant negative form of SarI (SarI^{H74L}::YFP) [24, 25] to specifically block the transport between the ER and vacuole. It has been already documented that PSI-A is able to bypass this blockage and accumulate in the vacuole [8]. Here we show that PSI-B::mCherry is more affected if this pathway is

Preprints (www.preprints.org) | NOT PEER-REVIEWED | Posted: 2 August 2019 doi:10.20944/preprints201908.0027.v1

Peer-reviewed version available at Plants 2019, 8, 312; doi:10.3390/plants8090312

blocked as it gets retained in ER-Golgi compartments (Figure 1D – arrows), despite some protein still being able to accumulate in the vacuole.

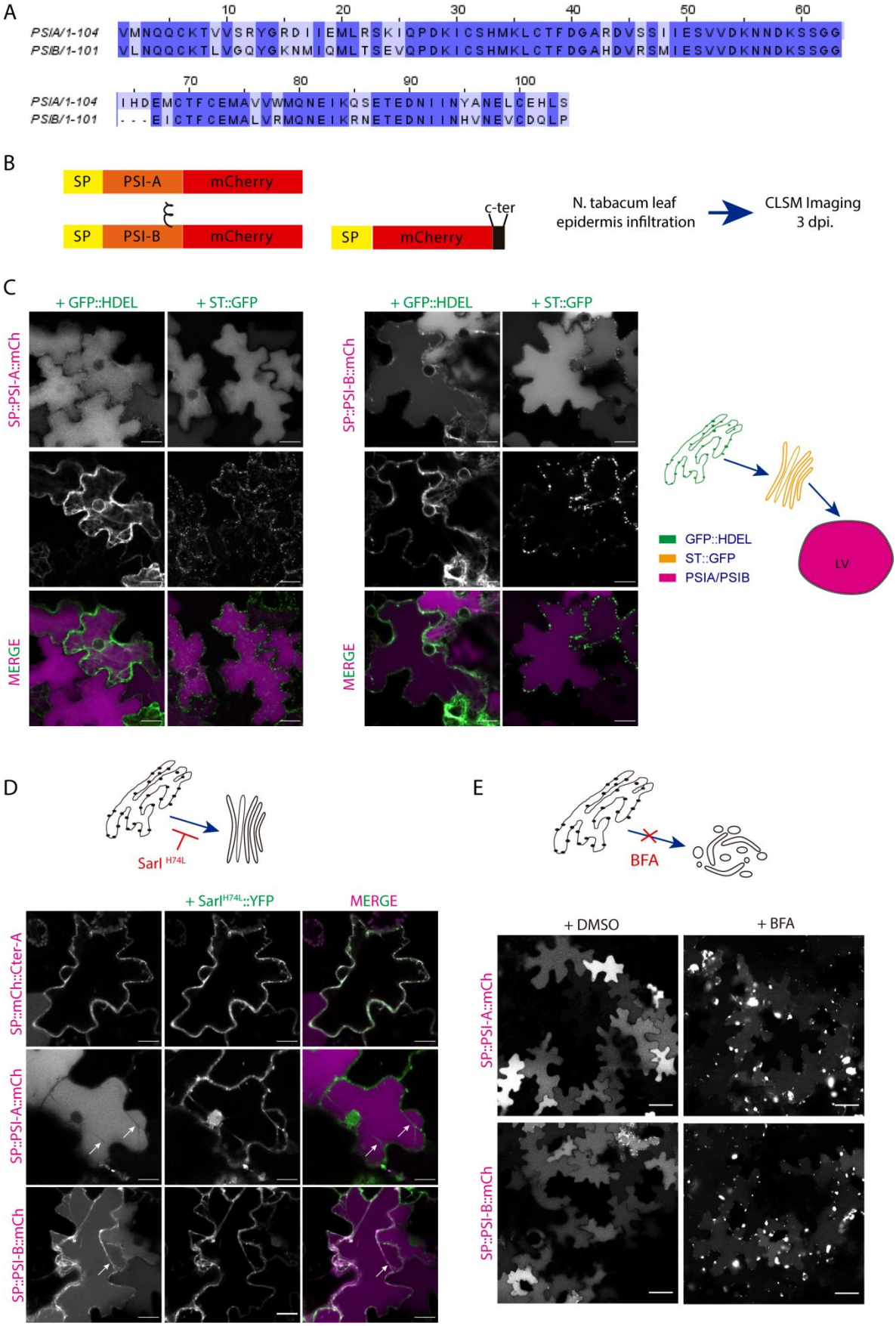

Figure 1: Expression of PSI-A and PSI-B in *N. tabacum* epidermal cells reveals subtle differences between the two. A) Alignment of cardosins A and B PSIs, showing the identity between them. B) Schematic of the constructions designed for this study and the methodology employed. C) Co-expression of PSI-A and PSI-B with the ER marker GFP::HDEL and the Golgi marker ST::GFP. Single images for both channels and the composite image are provided. D) Co-expression of PSI-A and PSI-B with the dominant negative mutant SarI^{H74L}::YFP. SP::mCh::C-terA was used as a positive control for the efficiency of the mutant SarI. Arrows indicate cytoplasmic/ER strands. E) Expression of PSI-A and PSI-B followed by Brefeldin A treatment. DMSO was used as a negative control of the experiment. All observations and images were acquired 3 days post-infiltration. Images were analyzed and processed using ImageJ/Fiji software. Scale bars: C and D - 20μm; E - 50μm.

This indicates that, despite the high homology between these two domains, there must exist a specific characteristic driving this Golgi-independent trafficking of PSI-A. One feature that immediately stands out is the presence of a glycosylation motif in PSI-B (NetNGlyc 1.0 Server prediction - http://www.cbs.dtu.dk/services/NetNGlyc/ - Figure 2A, red box) that is absent in PSI-A, which we decided to explore in more detail. Additionally, we did a parallel assay using BFA [26] to block the ER-to-Golgi transport (Figure 1 E). BFA is known to inhibit the function of COPI resulting in impaired ER export and disruption of the ERES (ER-export sites), thus inhibiting vesicle budding or fusion [27]. The results obtained show accumulation of both fusion proteins in large aggregates (most probably BFA compartments [26]) despite some mCherry fluorescence also being detected in the vacuole (Figure 1E). The interpretation of these results led us to consider that BFA's effect in PSI-mediated trafficking is more pronounced, probably because BFA affects the PSI export from the ER, by a still unknown mechanism. SarI dominant negative mutant action is more specific, and the ER morphology is much less affected than with BFA [28]. To corroborate these results, we also co-expressed our constructs with the dominant negative version of RabD2a – RabD2a^{N121I} [29] obtaining the same results (data not shown).

2.2. N-linked glycosylation modulates PSI-mediated sorting

To investigate in more detail the effect of glycosylation in PSI-mediated trafficking we decided to invert the glycosylation status of the PSIs by introducing a glycosylation motif in PSI-A (SETE>NETE – PSI-A^{S86N}) and removing the same motif in PSI-B (NETE>SETE – PSI-B^{N82S}) by site-directed mutagenesis (Figure 2A). Western blot analysis using a monoclonal anti-mCherry antibody (Figure 2B) of the glycosylated and non-glycosylated PSIs show differences in the proteins' migration patterns since PSI-B does not migrate as far as PSI-A in the gel. Since PSI-A and B molecular weight is roughly the same this must be related with the existence of post-translational modifications in PSI-B. In fact, the non-glycosylated form of PSI-B migrates further in the gel than the native one (Figure 2B), indicating that the presence of the glycan could be, at least in part, responsible for this difference in gel migration. Accordingly, the glycosylated version of PSI-A does present a band with a higher molecular weight than the native PSI-A, indicating the presence of a glycan. To add more data to this discussion, we performed an EndoH assay using the native and mutated PSI forms. EndoH is an enzyme that removes the high-mannose glycans that are added in the ER but not the complex glycans generated in the Golgi. The output in a Western blot, would be a shift in molecular weight upon digestion with EndoH. As expected, no shift is visible in the blot (Figure 2C) for either PSI-A or PSI-B mutated version, since they are not predicted to be glycosylated. In contrast, for the PSI-A glycosylation mutant a decrease in apparent molecular weight between the untreated and treated samples is quite evident (Figure 2C, arrow), consistent with the presence of high-mannose glycans acquired in the ER. Native PSI-B however, is likely to possess complex type glycans, modified in the Golgi, as it does not seem to be affected by EndoH treatment as no shift can be observed in the blot. It is worth to point out, that even the non-glycosylated form of PSI-B has an apparent higher molecular weight than both the native and the mutated version of PSI-A, an indication that other modification, rather than N-glycosylation, might exist in this domain.

Preprints (www.preprints.org) | NOT PEER-REVIEWED | Posted: 2 August 2019 doi:10.20944/preprints201908.0027.v1

Peer-reviewed version available at Plants 2019, 8, 312; doi:10.3390/plants8090312

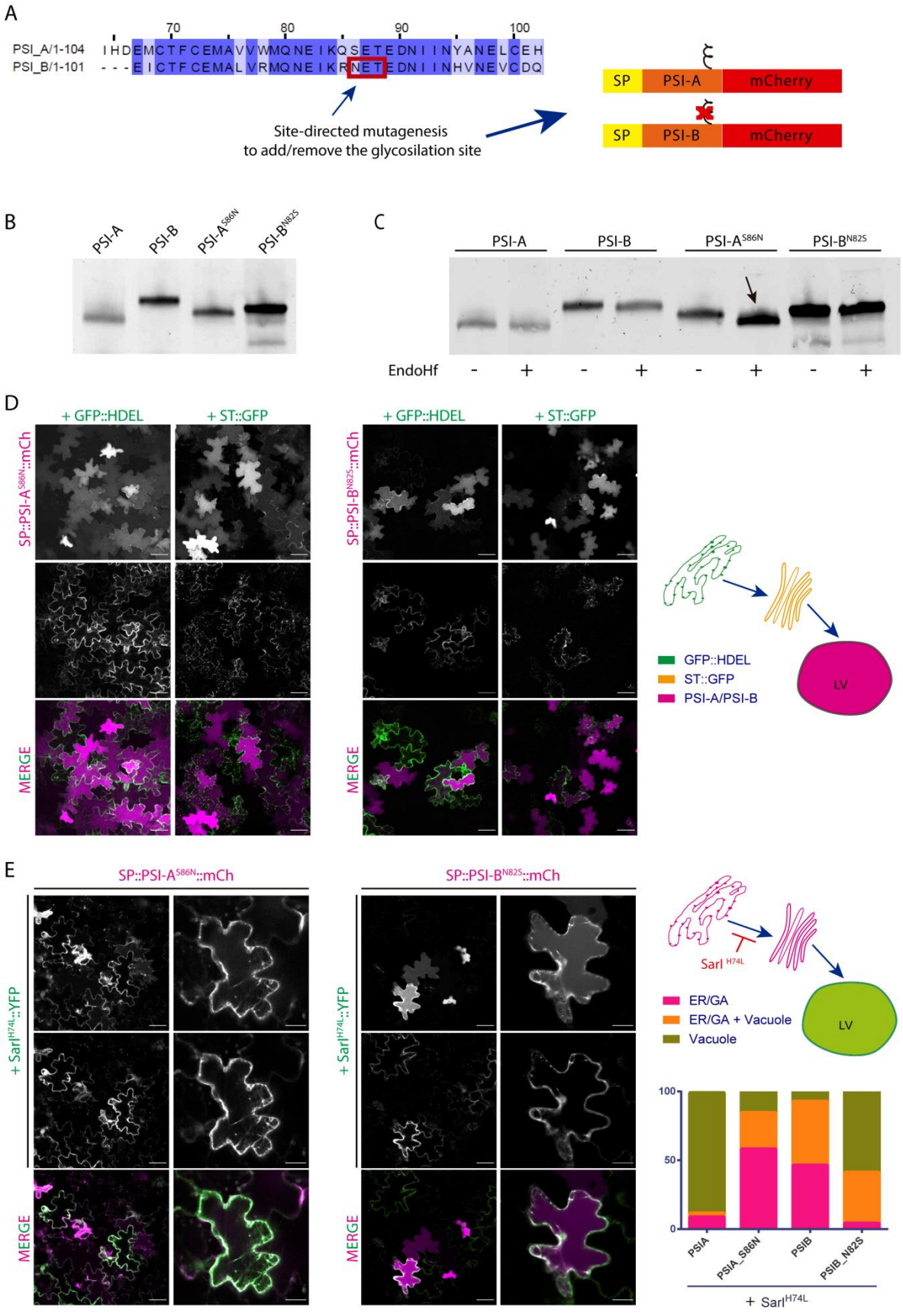

Figure 2: Expression of PSIs' glycosylation mutants in *N. tabacum* epidermal cells highlights a putative role for N-glycosylation in trafficking. A) Alignment of cardosins A and B PSI showing the glycosylation motif on PSI-B – red box – and a schematic of the mutated versions produced. B) Western blot of the native and mutated versions of the PSIs evidencing the differences in migration between them. C) Endoglycosidase H assay result of all PSIs. Note the shift in protein migration for PSI-A^{S86N} (arrow). D) Co-expression of PSI-A^{S86N} and PSI-B^{N82S} with the ER marker GFP::HDEL and the Golgi marker ST::GFP.

Single images for both channels and the composite image are provided. E) Co-expression of PSI-A^{S86N} and PSI-B^{N82S} with the dominant negative mutant SarI^{H74L}::YFP indicate differences in the sensitivity of the mutants to this blockage. Comparison between the mutated and native PSI forms under the effect of SarI^{H74L}::YFP is presented in the graph. All observations and images were acquired 3 days post-infiltration. Images were analyzed and processed using ImageJ/Fiji software. Scale bars: D – 50 μm; E – left panels, 50 μm and right panels, 20 μm.

Next, we analyzed the expression of PSI-A^{S86N} and PSI-B^{N82S} mutants by confocal microscopy together with ER and Golgi markers. Three days after tobacco cells transformation glycosylated PSI-A::mCherry and non-glycosylated PSI-B::mCherry fusions were mostly observed in the vacuole (Figure 2D). However, a closer look discloses some protein still in the ER possibly still in transit to the vacuole. In the same way to what was done for the native form of PSIs, SarI^{H74L} dominant negative mutant was used to block the ER-to-Golgi trafficking (Figure 2E). When co-expressed with the dominant-negative mutant, PSI-A^{S86N} no longer reached the vacuole, starting to be retained in early secretory compartments. De-glycosylated PSI-B, in contrast, was able to reach the vacuole but not as efficiently as the native non-glycosylated PSI-A as some protein is being retained in the ER when co-expressed with the mutated form of SarI. Given the novelty of the results obtained and to get a better view of the microscopic observations, quantitative analysis was performed on the results from the observation of more than 90 cells from three independent experiments. For the quantification it was considered that the total number of cells with fluorescent signal define a 100% value and among this population the different localization patterns were then scored. Data obtained from the quantification of fluorescence patterns reflects the subcellular localization observed in confocal microscopy analysis (Figure 2F).

2.3. PSI domains maintain their sorting capacity, independently of the overall AP structure

Different PSI domains are linked with different vacuolar sorting routes in the plant cell and this feature is probably related with their physiological roles (or the role of the aspartic proteinase they belong to) in the native plant, raising the question whether they can retain their sorting properties if in the context of the entire protein. To assess that we tested the expression and sorting of cardosin A, cardosin B and the chimaeras cardosin A with cardosin B PSI (CardosinA::PSI-B) and cardosin B with cardosin A PSI (Cardosin B::PSI-A) (Figure 3A and Sup. Figure 1A).

Knowing that the carboxy termini-mediated vacuolar trafficking is dominant over PSI-mediated trafficking in cardosin A [8], and since we were primarily interested in observing PSI-mediated trafficking dynamics, we began this work by removing the ctVSD from all tested chimaeras (Figure 3A). Upon removal of the C-terminal peptides the vacuolar accumulation pattern remained observable for all tested fluorescent fusion proteins, indicating that both PSI domains are sufficient for directing either of these aspartic proteases to the lytic vacuole, and further confirming the exchangeability of these domains between aspartic proteinase molecules Figure 3B).

In order to further dissect the specific pathways each of these constructs followed towards the vacuole, we expressed each one of them in cells undergoing blockage at specific points of the secretory pathway. Cardosin A behavior has already been thoroughly explored at the ER-Golgi level, with a clear difference between cardosin A and its truncated version (Cardosin AΔC-ter) being apparent. In particular, the removal of its carboxyl terminus results in an acquired insensitivity towards SarI^{H74L} and RabD2a^{N121I} blockage of COPII vesicle formation, a phenomenon that has been attributed to the route mediated by this AP's PSI domain [8]. On the other hand, removal of cardosin B C-terminus (Cardosin BΔC-ter) did not result in a Golgi-bypass capability, with the fluorescence becoming accumulated within the ER network upon co-expression with the dominant negative mutant form of SarI (Figure 3C). A similar behavior could be observed with the Cardosin A::PSI-BΔC-ter constructs.

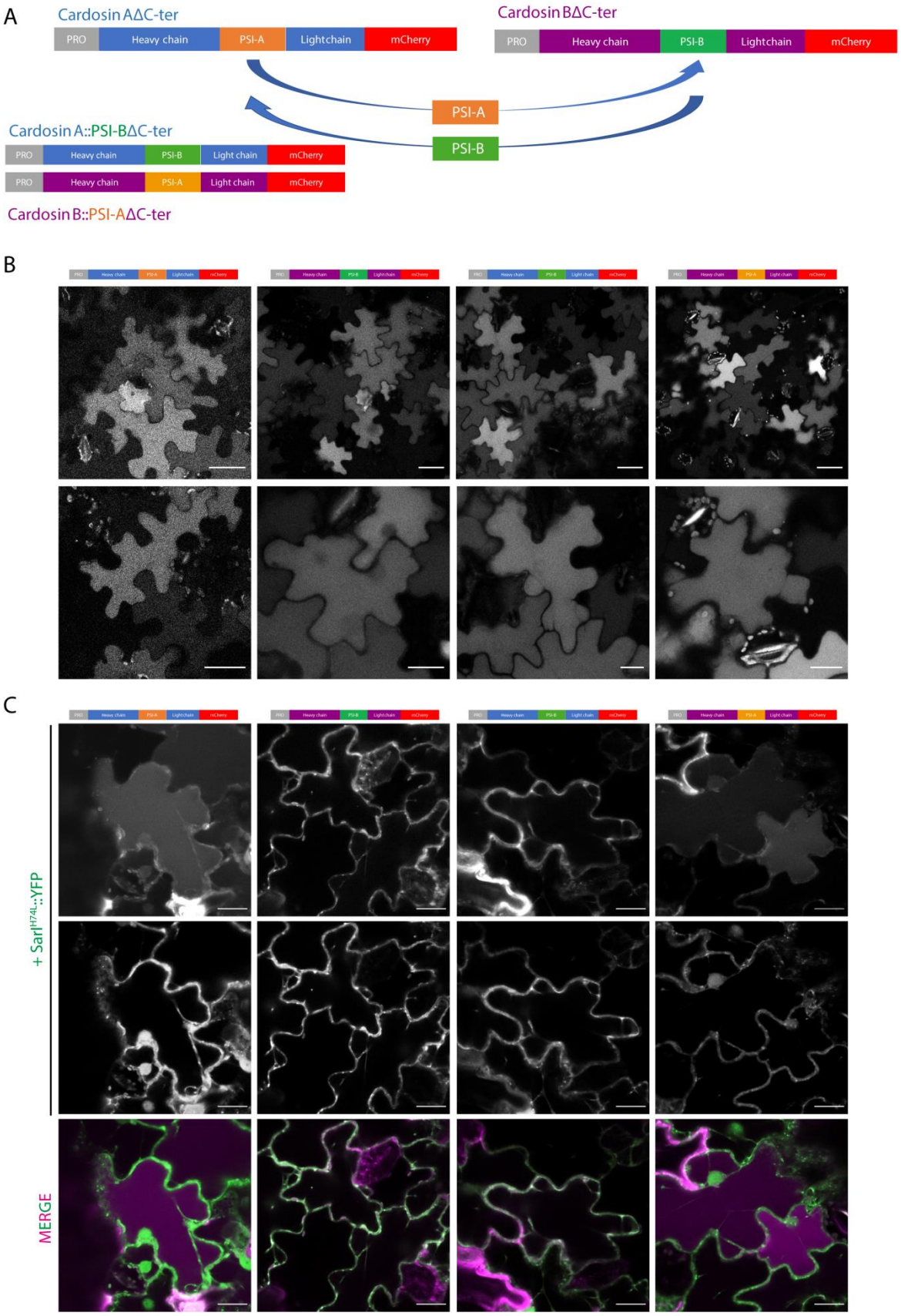

Figure 3: Subcellular localization of cardosins A and B and PSI-swapped version in *N. tabacum* epidermal cells. A) Schematic representation of the constructs used in this assay. B) Expression in tobacco epidermal cells evidencing the vacuolar localization of all constructs. C) Co-expression of cardosins constructs with the dominant negative mutant SarI^{H74L}::YFP. Note the differences in vacuolar accumulation depending on the PSI domain present. All observations and images were acquired 3 days post-infiltration. Images were analyzed and processed using ImageJ/Fiji software. Scale bars: B – upper panels, 50 μm and lower panels 20 μm; C – 20 μm.

Co-expression of this protein with the dominant negative mutant SarI^{H74L}, or the small GTPase RabD2a^{N121I} (not shown), resulted in an ER accumulation pattern (Figure 3C), suggesting that this construct must pass through the Golgi before reaching the vacuole. These observations allow us to conclude that (i) PSI-B domain retains its functionality as a VSD in the heterologous proteins tested, and that (ii) it directs aspartic proteases to the vacuole through a Golgi dependent pathway, whether it is expressed alone or in the context of an AP. Contrary to what could be observed with the truncated cardosin BΔCter, Cardosin B::PSI-AΔC-ter demonstrated the same insensitivity towards the ER-Golgi blockage as could be observed with all other reporters containing the PSI A determinant, accumulating in the vacuole even when co-expressed with either SarI^{H74L} (Figure 3C) or RabD2a^{N121I} (not shown). This result confirms that exchanging the PSI domains between both aspartic proteases results in a shift in terms of vacuolar sorting route followed by the reporter protein.

2.4. Post-Golgi trafficking of PSI-B might be modulated by protein structure

After having determined cardosin B PSI functionality as a VSD in both cardosins A and B sequences, we aimed at further dissecting its dynamics as an isolated domain, at the post-Golgi level, as previously reported for cardosin A PSI domain [8]. To this end, we co-expressed PSI-B::mCherry with the dominant negative version of the small GTPase RabF2b - RabF2b^{S24N}, which has been previously described as being capable of impairing protein sorting between the Golgi and the PVC [29] (Figure 4B). The results were compared to those obtained for PSI-A::mCherry, which is known to bypass the Golgi in its sorting towards the lytic vacuole and thus not affected by post-Golgi blockage events. As positive control, we used the previously described RabF2b-sensitive cardosin A C-terminal peptide [8], which was infiltrated in a separate region of the same leaf as the experimental constructs. We observed accumulation of the PSI-B::mCherry fluorescence at the periphery of the cell when co-expressed with the dominant negative form of RabF2b (Figure 4C), suggesting a PVC mediated pathway. We proceeded with the dissection of the vacuolar sorting route followed by the APs under direct control of the PSI B domain. Under these experimental conditions, the truncated reporters Cardosin AΔC-ter and Cardosin B::PSI-AΔC-ter accumulated in the vacuole when co-expressed with RabF2b^{S24N}, which was expected given the PSI-mediated Golgi-bypass route suggested for these chimaeras. More unexpected were the results obtained for PSI B-mediated vacuolar sorting: when trafficking was blocked at the post-Golgi level, PSI B-mediated vacuolar sorting remained unchanged, as can be observed by permanent vacuolar accumulation of the Cardosin BΔC-ter and Cardosin A::PSI-BΔC-ter chimaeras (Figure 4D). These observations contrast with the ones obtained for the isolated PSI-B domain, that is not able to overcome this blockage.

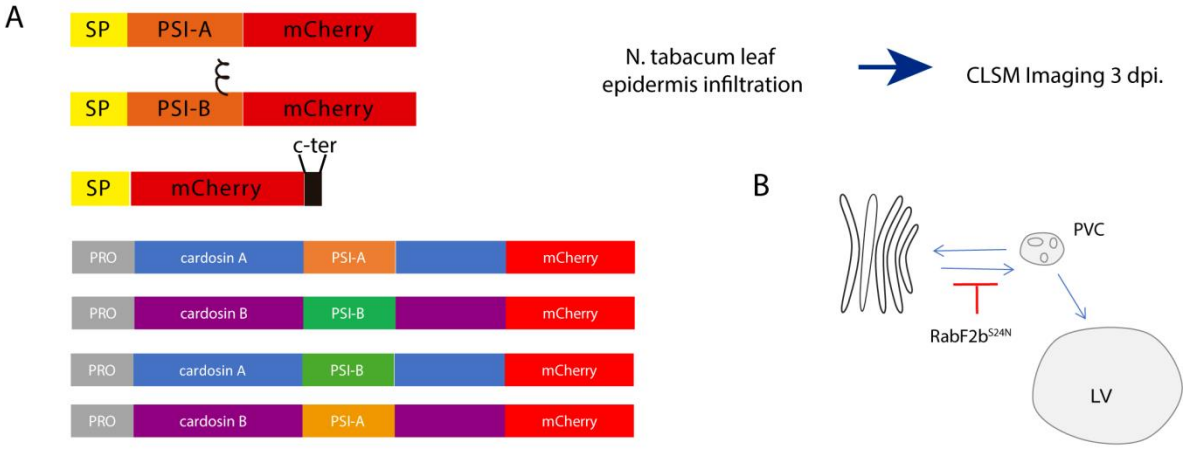

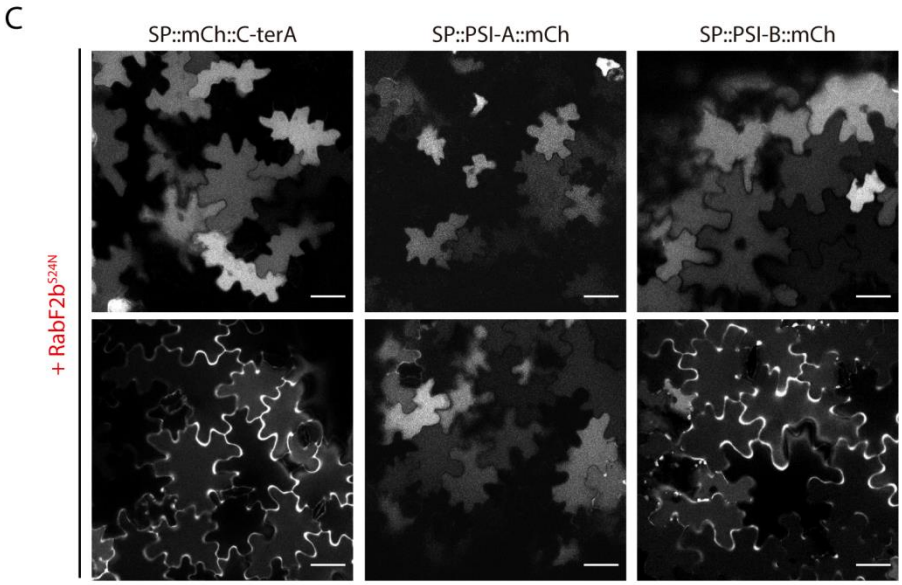

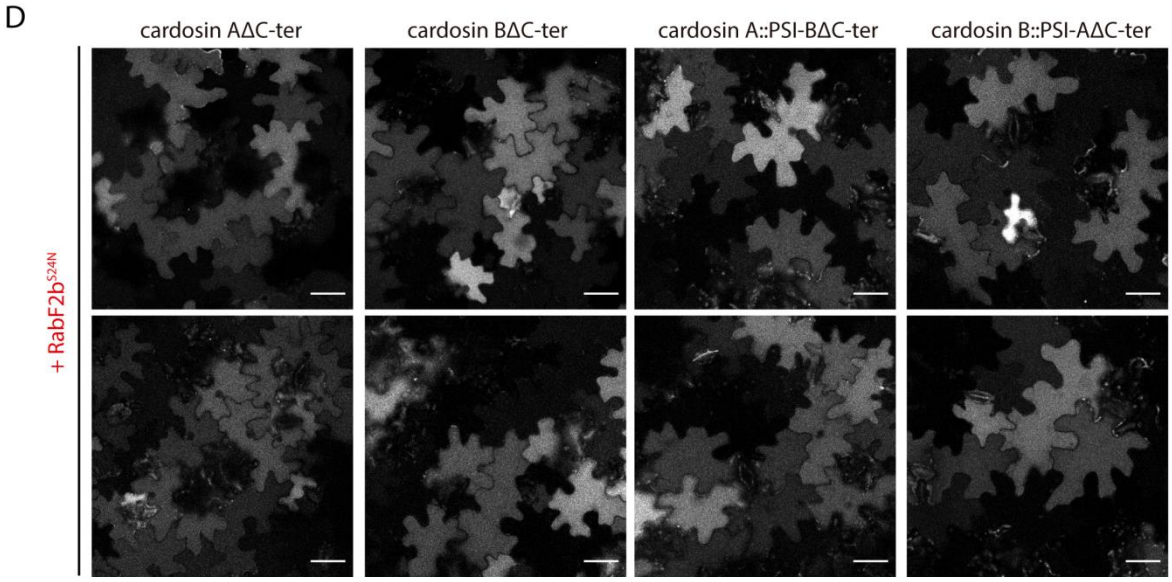

Figure 4: Co-expression of isolated PSIs and cardosins constructs with the dominant negative mutant of RabF2b. A) Schematic drawing of the constructs used in this assay. B) Drawing representative of RabF2b^{S24N} effect in cells. C) Co-expression of PSI-A and PSI-B with the dominant negative mutant RabF2b^{S24N}. SP::mCh::C-terA was used as a positive control for the efficiency of the mutant. Note the accumulation in the cell wall in the positive control and PSI-B, but not for PSI-A. D) Co-expression of RabF2b^{S24N} with cardosins constructs show that all the constructs are insensitive to the blockage of this

specific pathway. All observations and images were acquired 3 days post-infiltration. Images were analyzed and processed using ImageJ/Fiji software. Scale bars: 50 μm.

2.5. Proof of concept: the Soybean PSIs case

At least five aspartic proteinases have been identified in the soybean plant [*Glycine max* (L.) Merr.] SoyAP1 and soyAP2 were chosen as two representative soybean aspartic proteinases, due to the high similarities between their amino acid sequences and localization. Both have been isolated and characterized [31]. Like cardosins, soyAPs accumulate in different organs in the plant and show different localization and expression patterns. Furthermore, both have a PSI domain and has been suggested by Terauchi and co-workers (2006) that soyAP2-PSI is relevant for protein sorting, but not soyAP1-PSI [19]. Given our work on cardosins PSIs we became interested in these proteins given their potential as vacuolar sorting determinants and because they share the same glycosylation pattern as cardosins PSIs: PSI-1 is glycosylated, while PSI-2 is not (Figure 5A – red box). We isolated the two Soybean PSIs and cloned them in frame with the chitinase signal peptide and mCherry (Figure 5B), in a similar manner as the cardosins PSIs were designed. The first step to analyze and compare the behavior of the soy PSIs was to do a Western blot and Endo-H experiment to see if they behaved as the cardosins' PSI domains. Two characteristics immediately stood out in the blot: the PSI-2 was expressed at lower levels than PSI-1 (equal loadings were used) and there were no migration differences between the two PSIs as was observed for PSI-B (Figure 5C). Regarding glycosylation status, for PSI1 a shift could be observed upon treatment with Endo H, consistent with the presence of high-mannose glycans. The result obtained contrasts with the one observed for PSI-B, whose glycans are of the complex type (Figure 2C). In this case, either the glycosylation sites are not accessible to Golgi-modifying enzymes, the protein leaves the Golgi in a very early step before Golgi enzymes are able to modify the glycans, or the protein bypasses the Golgi.

Next, we proceeded to evaluate the sorting ability and trafficking pathway of SP::PSI-1::mCh and SP::PSI-2::mCh. After 3-days of transient expression in tobacco leaves both PSI-1 and PSI-2 accumulate in the vacuole (Figure 5D). In some cells mCherry fluorescence is visible accumulating at the cell periphery, but this is probably an artefact of overexpression, since increasing or decreasing the OD of the infiltrated construct resulted in more or less cells, respectively, with fluorescence in the apoplast (not shown). Co-expression with SarI^{H74L}, which impairs trafficking between the ER and Golgi, revealed differences between the two PSIs, as PSI-1 (glycosylated) is not able to reach the vacuole, becoming retained in the early endosomal compartments, while PSI-2 is not affected by this blockage (Figure 5E). Moreover, treatment with BFA resulted in accumulation of both constructs in BFA body-like structures (Figure 5F), regardless of some protein being detected in the vacuole in the case of PSI-2. The results obtained with the soyPSIs are quite similar to the ones observed for cardosins' PSIs, in terms of accumulation and glycosylation effect, giving us extra confidence in the hypothesis considered.

Preprints (www.preprints.org) | NOT PEER-REVIEWED | Posted: 2 August 2019 doi:10.20944/preprints201908.0027.v1

Peer-reviewed version available at Plants 2019, 8, 312; doi:10.3390/plants8090312

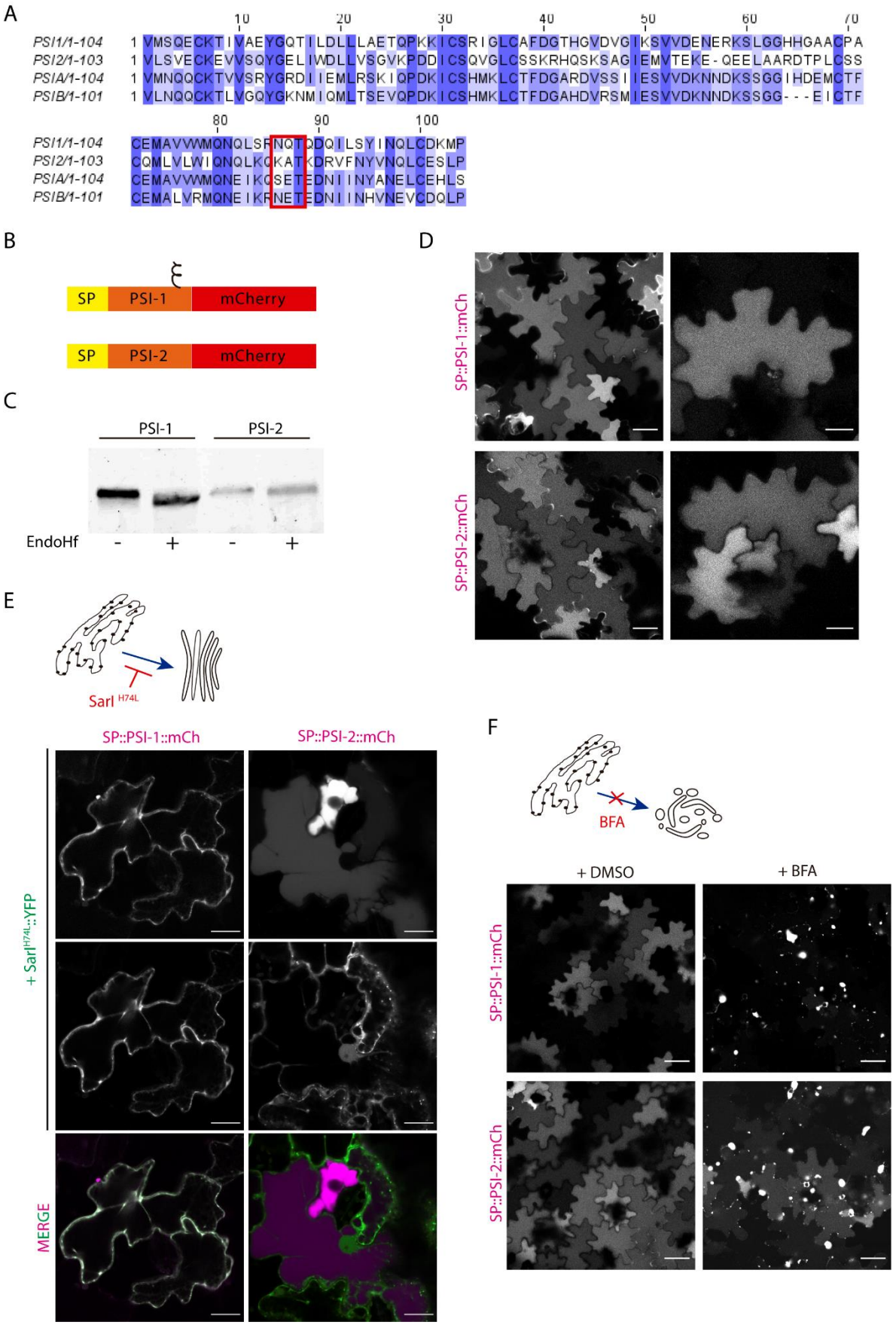

Figure 5: Expression of Soybean PSIs in *N. tabacum* epidermal cells present the same dichotomy as cardosins' ones. A) Alignment of Soybean (PSI-1 and PSI-2) and cardosins (PSI-A and PSI-B) PSIs. The sequence conservation is not high, but PSI-1 is predicted to be glycosylated as PSI-B – red box. B) Schematic of the two constructs designed for the experiment. C) Blot obtained after an endoglycosidase H assay for PSI-1 and 2, where a shift-down in the band corresponding to PSI-1 is evident.

D) Vacuolar localization of both constructs in tobacco epidermal cells. E) Co-expression of PSI-1 and PSI-2 with the dominant negative mutant SarI^{H74L}::YFP indicates differences in the sensitivity of the mutants to this blockage. F) Expression of PSI-1 and PSI-2 in tobacco cells followed by Brefeldin A treatment. DMSO was used as a negative control of the experiment. All observations and images were acquired 3 days post-infiltration. Images were analyzed and processed using ImageJ/Fiji software. Scale bars: D – left panels 50 μm, right panels 20 μm; E - 20 μm; F - 50 μm.

3. Discussion

Cardosins are well characterized aspartic proteinases extracted from the vascular plant *Cynara cardunculus* [32, 33]. Two different, yet related, proteinases were isolated – cardosins A and B – and they have been extensively studied over the years both in the native and heterologous systems [8, 12, 34, 35, 36, 37]. Each of these enzymes is synthesized as a precursor and undergoes different cleavages along the endomembrane system in order to acquire its mature form, composed of a heavy and light chains. One domain that is cleaved out during this process is an insert of 100 amino acids termed the Plant Specific Insert (PSI). The relevance of this domain for the aspartic proteinase function has been widely discussed mostly because it is only present in some aspartic proteinases [38, 39]. Several roles have been attributed to this particular domain namely given its ability to interact with lipid membranes and its putative antimicrobial activity. A number of studies depict these possibilities using PSIs isolated from different plants and it has been proven that this domain can modulate the behavior of model membranes [40] and is also able to induce membrane permeabilization and thus release vesicle contents [14]. This ability is closely related to its antimicrobial activity: a study with *Solanum tuberosum* aspartic proteinase PSI showed that it enhances *Arabidopsis thaliana* resistance against *Botrytis cinerea* infection [20] and another report using the same PSI showed that it is cytotoxic against Gram-negative and Gram-positive bacteria [17].

This report focuses on another ability of the PSI that is the sorting of proteins to the vacuole, a characteristic that could in fact be related to the functions mentioned above. Therefore, understanding the mechanisms of PSI-mediated sorting and trafficking inside the cell might as well help elucidate some of its other functions.

3.1. A role for PSIs in vacuolar sorting

The majority of aspartic proteinases containing a PSI domain accumulate in the vacuole and the role of the PSI in vacuolar sorting has long been discussed and was effectively tested in different studies using cardosins and soybean aspartic proteinases [8, 19, 21]. The study of the vacuolar sorting capability of the PSI in the case of cardosins is challenged by the presence of the C-terminal VSD also present in the precursor form of the enzyme. In the report by Pereira *et al* (2013) it was shown that as long as the typical C-terminal VSD is carried by the protein, the PSI domain is not necessary for the protein to reach the plant vacuole. However, in the absence of C-ter VSDs, the PSI domain acts as a true VSD, being sufficient for correct vacuolar targeting of aspartic proteinases [8]. This is true for the two PSIs studied – cardosin A's PSI and cardosin B's PSI – but a major difference was observed by our team and further explored in this study using SarI^{H74L} coupled to a YFP, allowing the direct visualization of the cells co-expressing the two proteins. While PSI-B uses a COPII-dependent pathway from the ER to the Golgi, the PSI-A pathway to the vacuole is independent of COPII carriers thus not being affected by the blockage provided by SarI^{H74L}. Comparing the effect of co-expressing SarI^{H74L} with cardosin A C-terminal peptide fusion with mCherry or with PSI-B::mCherry fusion, the results are significantly different as some PSI-B::mCherry fluorescence in the vacuole is still visible, while all the C-terminal fusion protein is retained in early compartments. It is fair to say that some of the PSI-B::mCherry protein is independent of COPII transport or that the effect of SarI^{H74L} only delays its accumulation in the vacuole. Nevertheless, the differential accumulation of PSI-A and PSI-B when co-expressed with the dominant negative form of SarI is clear– PSI-A accumulates in the vacuole not being affected by the blockage while PSI-B mCherry fusion is retained in the ER. The question raised at this point was: what is the difference between the two PSI domains underlying this differential behavior? The two PSIs are quite similar in terms of protein sequence and the one feature that stands

out upon analysis, is the presence of an N-linked glycosylation site in PSI-B. We therefore hypothesized that post-translational modification could be a key component in determining the route to be taken by the PSI-driven targeting. In fact, studies on phytepsin [21] revealed that the transport of this AP is COPII-mediated and that the PSI domain was essential for phytepsin's transport through the Golgi. Interestingly, as for the most common APs (including cardosin B), phytepsin has a conserved glycosylation site in the PSI domain.

3.2. The significance of glycosylation in sorting

The role of glycosylation in the vacuolar routes taken by proteins in the secretory pathway has long been discussed, in particular involving Golgi bypass [7, 41, 42]. In order to understand how the glycosylation of the PSI domain affects its trafficking route we introduced an artificial glycosylation site in cardosin A's PSI to obtain a structure similar to the one of cardosin B's and to evaluate if the glycosylation would influence the route taken by PSI-A. The opposite was obtained for PSI-B, where the glycosylation motif was removed and replaced with the amino acid present in cardosin A's PSI sequence. In contrast to the non-glycosylated PSI that accumulates in the vacuole despite the ER-to-Golgi blockage, the mutated version was retained in the early compartments when co-expressed with SarI^{H74L}. Furthermore, the non-glycosylated form of PSI-B was no longer sensitive to the ER-to-Golgi blockage, being able to accumulate in the vacuole even when co-expressed with SarI^{H74L}. These results unleash a debate about the relevance of N-glycosylation in protein trafficking. It has been previously proposed that N-glycosylation is not determinant for the correct trafficking of the vacuolar protein, leading instead to a delay in the trafficking [43, 44]. Here we show that the glycosylation may indeed be important for the route taken by proteins, in particular in what concerns their passage through the Golgi. This is true for cardosin A's PSI, as the difference in sensitivity to ER-to-Golgi blockage of the non-glycosylated and glycosylated form is striking. In the case of PSI-B, however, the results obtained in this report are not as clear cut and a more complex interpretation may be needed. The non-glycosylated form of the protein, despite being able to accumulate in the vacuole, is also detected in the ER. In fact, the effect of the co-expression with SarI dominant negative mutant in the vacuolar accumulation of PSI-B::mCherry is not so different for the glycosylated and non-glycosylated versions. In addition, we have also shown that PSI-B migrates in the Western blot at a higher molecular weight than the PSI-A, and this higher molecular weight is maintained after endo-H digestion. All these observations clearly indicate that there must be another post-translational modification interfering with the sorting and trafficking of PSI-B, that must be explored.

3.3. Soy PSIs case – another piece of evidence

As previously commented in this report, the number of aspartic proteinases containing a PSI is lower than the typical or nucellin-like aspartic proteinases [38, 39]. More interesting is the fact that most of the PSIs have the glycosylation motif, like cardosin B's PSI and only a few are not glycosylated. Terauchi and co-workers (2004, 2006) [19, 31] isolated and characterized two aspartic proteinases from soybean – SoyAP1 and soyAP2 – and also discuss the role of the PSI in the vacuolar targeting of these enzymes. Interestingly, analysis of the soy PSIs sequence made it apparent that they share the same dichotomy as cardosins' PSIs: one is glycosylated and the other is not. As a proof of concept, we isolated the soy PSIs and ran the same experiments as for cardosins' PSIs to check if their trafficking would be affected. Subcellular localization of Soy PSI::mCherry chimeric proteins show accumulation in the vacuole, establishing that both Soy PSI domains are VSDs and contain all the necessary information for vacuolar sorting. Furthermore, and like cardosins' PSIs, soy PSIs show differential sensitivity to ER-to-Golgi blockage when co-expressed with SarI^{H74L}, in a glycosylation-dependent manner. Although it was suggested in the report by Terauchi and co-workers [19] that soyAP1's PSI was not involved in vacuolar sorting events, the data obtained in this study clearly shows this is not the case. Probably, in the context of the enzyme, the soy PSI is in a conformation that does not allow the vacuolar accumulation of the protein, or it might be subjected to the type of hierarchical regulation that was previously described for cardosin A's VSDs [8]. It is also possible

that the importance of the PSI in the vacuolar sorting information depends on the plant developmental stage, or the organ/cell type where it is being expressed in. In fact, the authors show that removal of the PSI domains altered the APs targeting to the lytic vacuole, but not to the protein storage vacuole. The PSI may, therefore, act as vacuolar signal only in specific conditions or developmental stages. Taken together the results obtained with the cardosin and soy PSIs allows us to assume that glycosylation may play an important role in the sorting and trafficking of proteins or at least influence the way proteins leave the ER.

3.4. Cardosin B PSI: One VSD, multiple pathways?

In former studies, Pereira and colleagues pointed out that the occurrence of multiple VSDs in cardosins (and atypical APs in general) could be related to regulatory mechanisms employed by plants in order to increase these proteases' functional diversity in different types of cells, tissues and/or developmental stages [5, 8]. Our results with PSI B-mediated sorting may come as further confirmation of this hypothesis, as we have observed a differential behavior between vacuolar sorting mediated by this domain on what could be described as a case-by-case mechanism. Isolated PSI-B fused to the mCherry fluorescent reporter was efficiently directed towards the vacuole in a RabF2b-dependent pathway, similar to what was observed with intact cardosins A and B [8, 35]. Integration of the PSI-B domain in an entire cardosin structure, independent of which cardosin was tested, however resulted in a different dynamic behavior as vacuolar sorting shifted from RabF2b-dependent to RabF2b-independent for PSI B-mediated vacuolar sorting. This observation is somewhat surprising, as it seems to imply that the vacuolar trafficking pathway followed by this domain is somehow determined by its overall three-dimensional structure, without compromising its VSD status or efficiency. This result came as a yet further confirmation that plant APs possess multiple VSDs capable of vacuolar sorting through different routes, and that despite similar three-dimensional structures, different PSI domains possess different specificities in terms of protein sorting to the vacuole. Given the importance of protein folding and three-dimensional structure in PSI-mediated functionality [14], it would be feasible to assume that isolation of this domain could give different results. This observation seems to imply that structural changes occurring in this domain could be modulating the route followed towards the lytic vacuole at the TGN-PVC level.

3.5. PSI-mediated sorting: an unconventional vacuolar sorting mechanism

In plant cells, the conventional route to the vacuole involves the ER, Golgi and the prevacuolar compartment [45]. However, in the last few years a more unconventional sorting route to the vacuole that bypasses the Golgi, has been described, which is the case of some vacuolar proteins such as Chitinase A [7] and several membrane proteins [46, 47]. However, the mechanisms underneath this Golgi-bypass are still unclear and are recently gaining attention [10, 48]. The Golgi-bypass is also the case for the route mediated by cardosin A's PSI. This domain is both sufficient and necessary to direct a secreted protein to the vacuole in an ER-to-Vacuole direct pathway. The mechanisms allowing Golgi bypass are currently unknown, but it is interesting to notice that it is not true for all PSIs. After resolving prophytepsin's crystallographic structure in 1999, Kervinen and coworkers identified a positively charged ring formed by residues from the PSI domain (Lys320, Lys400 and Arg415; preprophytepsin numbering) and the proteinase's light chain, that could correspond to a putative receptor binding site [48]. These residues are not all conserved between PSIs and we could hypothesize that the differential binding of PSIs with vacuolar receptors or ER-resident proteins could be the base of a Golgi-bypass mechanism. This hypothesis is also compatible with the idea that different PSI domains could have different sorting functions due to their glycosylation status, as the highly conserved N-linked glycan is inserted at the periphery of this positively charged ring (Asn399) and could be expected to either interfere or modulate protein-protein interactions taking place at this site. Our current data do not permit so far to determine the features needed for a PSI domain to act or not as VSDs nor to determine which route it will take. Considering that proteins delivered directly to the vacuole would have to be recognized at the ER level, testing the PSI interaction with several

ER proteins and even search for the existence of a PSI receptor, could be a clue to this question. In fact, the results from the BFA treatment presented here are an indication that alterations in ER/Golgi morphology or the re-localization of Golgi and ER-export sites' components (in this case induced by the drug) affect the vacuolar sorting mediated by PSI-A. In the presence of BFA PSI-A::mCherry fusion is mostly found in BFA-bodies not being able to accumulate in the vacuole as efficiently as before. It is a clear indication that the PSI-mediated Golgi-bypass is a process initiated and reliant on the ER. It would be exciting to explore in more detail the PSI-A mediated trafficking in order to gather more data and unveil the general mechanism behind this unconventional pathway.

4. Materials and Methods

4.1. Plasmids and vectors

All constructs used in this study were generated by Polymerase Chain Reaction (PCR) using specific primers (Table 1) and a proofreading DNA polymerase (Pfu DNA Polymerase, Thermo Scientific). Unmodified Cardosin A [34] and cardosin B [35] were used as templates for all PCR reactions for cardosins'-based cloning and Soybean AP 1 and 2 [31] as a template for PSIs 1 and 2. PCR fragments were initially cloned using the Zero Blunt® cloning kit (Invitrogen) and analyzed by restriction mapping. Positive clones were selected for sequencing using universal M13 primers (Eurofins MWG Operon, http://www.eurofinsdna.com/home.html). Cardosins' PSIs and mutated versions were then inserted into the XbaI and SalI (cardosin A/B-based constructs) sites of the binary vector pVKH18-En6::mCherry [50] and Soybean PSIs into XbaI and SacI sites of pMDC83 [51] for expression in plant cells. Specific details for each set of constructs are given below.

Table 1: Oligonucleotides and template DNA used to produce the constructs used along this project.

Construct to make	Oligonucleotide Fwd	Oligonucleotide Rev	Template DNA
SP::PSI-A^{S86N}::mCherry	GGATGCAAAACGOLGIAATCAA ACAAAACGAGACTGAAGATAAC	GTTATCTTCAGTCTCGTTTTGTT TGATTTCGTTTTGCATCC	SP::PSI-A::mCherry
SP::PSI-B^{N92S}::mCherry	GCAGAATGAAATCAAACGAAGC GAGACTGAAGATAACATAA	TTATGTTATCTTCAGTCTCGCTT CGTTTGATTTCATTCTGC	SP::PSI-B::mCherry
SP::PSI-1::mCherry	ACGTCGACTGTTATGAGCCAAG AATGCAAGACC	TTGTCGACGCACCACCTGCAG CACCACCGCTAGGCATTTTATC GC	SoyAP1
SP::PSI-2::mCherry	ACGTCGACTGTTCTCAGTGTCGA ATGTAAGGAAGTC	TTGTCGACGCACCACCACTTG GCAGGCTCTCAC	SoyAP2
PSI-A (for cardosin A::PSI-B::mCherry)	GTCATGAACCAGCAATGCAA	GGATAAGTGTTCACACAACTC	Cardosin A
PSI-B (for cardosin B::PSI-A::mCherry)	TTAAACCAACAATGCAAAACAT TGG	TTCTGCACTTGAAGTGGGTA	Cardosin B
Cardosin AΔPSI::mCherry	ACTTCATCTGAAGAATTACAAG	CCCGTTAGCGCCAATTGCATG ATT	Cardosin A
Cardosin BΔPSI::mCherry	TCGATAGTAGACTGCAATGG	AACCCCTTTTGCACCAATTG	Cardosin B
Cardosin A::mCherryΔc-ter	TCTAGAGCCGCCACCATGGGTA CCT	GTCGACGCTAGTAAATTGCCA TAATCAAACACTGTG	Cardosin A
Cardosin A::PSI-B::mCherryΔc-ter	TCTAGAGCCGCCACCATGGGTA CCT	GTCGACGCTAGTAAATTGCCA TAATCAAACACTGTG	Cardosin A::PSI-B
Cardosin B::mCherryΔc-ter	CATCTAGACTCGAGCCACCATG GGAACCCCAATCAAAGCAAACG	ACGTCGACTTTAACTTGCCATA ATCG	Cardosin B
Cardosin B::PSI-A::mCherryΔc-ter	CATCTAGACTCGAGCCACCATG GGAACCCCAATCAAAGCAAACG	ACGTCGACTTTAACTTGCCATA ATCG	Cardosin B::PSI-A

Cardosins' A and B PSIs: Constructs encoding for PSI-A and PSI-B tagged with mCherry at the C-terminal were already available [8] and were used as template to generate the glycosylation mutants. Modified primers were designed (Table 1) and mutated forms were obtained using site-directed mutagenesis technique with Pfu DNA Polymerase (Thermo Scientific) coupled to template digestion with DpnI (Fermentas).

Soy AP's 1 and 2 PSIs: SoyAP1 and SoyAP2 cDNA cloned into pBLUESCRIPT II SK were kindly provided by Terauchi and co-workers [31]. In order to obtain the isolated domains each PSI was amplified by PCR using a specific set of primers that introduced SalI sites flanking the PSI (Table 1) and allow cloning in frame with mCherry into the pMDC83 vector containing SP::mCherry (already available).

Cardosins' swapped PSI domains: To swap the PSI domains between cardosins A and B, they were PCR-amplified (Table 1) in order to delete their native PSI domains – CardosinΔPSI::mCherry – and the PSIs were also isolated by PCR. CardosinΔPSI::mCherry sequences were then ligated to the PSI fragments for obtaining the swapped PSI versions (CdAPSI-B and CdBPSI-A constructs). Additionally, reverse primers were designed in order to delete the cDNA sequences encoding the proteins' c-terminal peptides and allow in-frame cloning with mCherry - Cardosin A::PSI-B::mCherryΔc-ter and Cardosin B::PSI-A::mCherryΔc-ter. The same primer pairs were used to remove the c-terminal sequence from the un-modified cardosins constructs - Cardosin A::mCherryΔc-ter and Cardosin B::mCherryΔc-ter.

4.2. Plant Material

The analysis of the constructs produced was done using the method of *Agrobacterium tumefaciens* mediated infiltration of *Nicotiana tabacum* leaf epidermis. Seeds of *N. tabacum* cv. SRI Petit Havana were germinated in petri dishes on filter paper, moistened with water. After germination, seedlings were transferred to individual pots with fertilized substrate (SiroPlant) and maintained in a growth chamber with a photoperiod of 16 h light, 60 % humidity and 21 º C.

4.3. Transient expression in N. tabacum *leaves*

Agrobacterium tumefaciens GV3101::pMP90 was transformed by electroporation, screened by restriction mapping, and used for infiltration of *Nicotiana tabacum* L. cv. Petit Havana SR1, as described by Batoko *et al* [29] with the following modification – YEB medium was replaced with LB broth supplemented with 50 $\mu g.mL^{-1}$ kanamycin. For co-expression experiments, the bacteria harboring the different constructs were mixed prior to infiltration, with the titre adjusted to the required OD600. The used OD600 were as follows: 0.3 for the PSIs and cardosins' constructs and 0.15 for ST::GFP, GFP::HDEL, $SarI^{H74L}$::YFP and $RabF2b^{S24N}$.

4.4. Drug Treatments

BFA Treatment in leaves: At 36-40 h after infiltration with the desired construct, infected areas of the leaves were infiltrated with 50 μM BFA. The infiltrated areas were removed and left to float on the same solution for 2 hours, at 21 °C in the dark.

4.5. Protein Sample Extraction and Endoglycosidase assays

Protein extraction from leaf tissue was performed in the presence of two volumes of extraction buffer [50 mM sodium citrate, pH 5.5; 5% SDS (w/v); 0.01% BSA (w/v); 150 mM NaCl; 2% (v/v) β-mercaptoethanol and 10 μL of protease inhibitor cocktail (Sigma-Aldrich)] per 300 mg of tissue sample. The tissue was mechanically disrupted and boiled for 10 minutes. The samples were then centrifuged at maximum speed for 30 minutes at 4 ºC and the supernatant collected. For Endo-H assays (Endo-Hf, New England Biolabs), 5 μL of total protein extract was used in each reaction and the protocol provided by the supplier was followed.

4.6. Western Blot

SDS-PAGE was performed using a 12% polyacrylamide gel. 10μL of total protein sample was loaded on the gel, and 5 μL of PageRuler™ Plus Prestained Protein Ladder (Fermentas) was used as a protein molecular weight marker. After electrophoresis, the proteins were transferred to a nitrocellulose membrane with a Tris-glycine-methanol buffer. The membrane was blocked for 1 hour

in Tris buffered saline supplemented with 5% (w/v) skim milk, 1% (w/v) bovine serum albumin and 0.6% (v/v) Tween 20. A monoclonal antibody against mCherry (Milipore) was used at a 1:1000 dilution to probe the membrane at 4 ºC, overnight. Alkaline phosphatase conjugated secondary antibody (Vector) was used at a 1:1000 dilution for 1 hour at room temperature, and the proteins exposed with Novex AP Chromogenic substrate (Invitrogen), according to the manufacturer's protocol.

4.7. Confocal Laser Scanning Microscopy - Image acquisition and analysis

Images were acquired with an inverted SP2 (for single image acquisition) or SP5 (for co-localizations) Leica laser scanning microscope. Pieces of leaf were sampled from the infiltrated area in a random fashion and mounted in water. The 561 nm laser line was used for excitation of mCherry, whereas the 488 line was used for exciting GFP and YFP. Images were processed using ImageJ/Fiji software.

5. Conclusions

With this report we show that a post-translational modification like N-linked glycosylation can interfere with the sorting and trafficking of vacuolar sorting determinants to the vacuole as the non-glycosylated PSI's are able to bypass the Golgi and accumulate directly in the vacuole. This work also confirmed the role of PSI in protein sorting and a deeper study in its function as an unconventional vacuolar determinant will definitely shed some light on the understanding of the mechanisms behind unconventional sorting to the vacuole. Moreover, considering previous results and the data presented here, it is plausible to suggest that the PSIs' role in vacuolar targeting can be dependent on the specific function of the proteinase it is integrating and on the developmental stage and metabolic activity of the tissue it is expressed in.

Supplementary Materials: The following are available online at www.mdpi.com/xxx/s1, Figure S1: Subcellular localization of cardosins A and B and PSI-swapped version with the C-terminal vacuolar sorting signal present.

Author Contributions: Conceptualization, S.P. and C.P.; Funding acquisition, J.P.; Investigation, V.V., B.P., M.C. and C.P.; Methodology, V.V., B.P. and C.P.; Project administration, J.P.; Supervision, V.V., S.P. and C.P.; Validation, S.P.; Visualization, V.V. and B.P.; Writing – original draft, C.P.; Writing – review & editing, V.V., B.P., S.P. and J.P..

Funding: This research was supported by and in the frame of the scientific project PTDC/BIA-FBT/32013/2017, funded by FCT.

Acknowledgments: We thank Dr. Kaede Terauchi that kindly shared the cDNAs for SoyAP1 and soyAP2 with us. We also would like to thank the laboratory of Dr. Ian Moore and Prof. Chris Hawes for sharing the dominant negative versions of RabF2a and SarI used in this study.

Conflicts of Interest: The authors declare no conflict of interest.

References

1. Müller J., Mettbach U., Menzel D., and Samaj J., "Molecular dissection of endosomal compartments in plants.," Plant Physiol., vol. 145, no. 2, pp. 293–304, Oct. 2007. DOI: 10.1104/pp.107.102863
2. Robinson D. G., Jiang L., and Schumacher K., "The Endosomal System of Plants: Charting New and Familiar Territories," Plant Physiol., vol. 147, no. 4, pp. 1482–1492, Aug. 2008. DOI: 10.1104/pp.108.120105
3. Zouhar J. and Rojo E., "Plant vacuoles: where did they come from and where are they heading?," Curr. Opin. Plant Biol., vol. 12, no. 6, pp. 677–84, Dec. 2009. DOI: 10.1016/j.pbi.2009.08.004
4. Neuhaus J.-M. and Rogers J. C., "Sorting of proteins to vacuoles in plant cells," in Protein Trafficking in Plant Cells, Dordrecht: Springer Netherlands, 1998, pp. 127–144. DOI: 10.1007/978-94-011-5298-3_7
5. Pereira C., Pereira S., and Pissarra J., "Delivering of proteins to the plant vacuole-an update," Int. J. Mol. Sci., vol. 15, no. 5, 2014. DOI: 10.3390/ijms15057611

6. Vitale A. and Hinz G., "Sorting of proteins to storage vacuoles: how many mechanisms?," Trends Plant Sci., vol. 10, no. 7, pp. 316–23, Jul. 2005. DOI: 10.1016/j.tplants.2005.05.001
7. Stigliano E., Faraco, M., Neuhaus, J-M, Montefusco, A., Dalessandro, G., Piro, G., Di Sansebastiano, G-P, "Two glycosylated vacuolar GFPs are new markers for ER-to-vacuole sorting," Plant Physiol. Biochem., vol. 73, pp. 337–343, 2013. DOI: 10.1016/j.plaphy.2013.10.010
8. Pereira C., Pereira S., Satiat-Jeunemaitre B. and Pissarra J., "Cardosin A contains two vacuolar sorting signals using different vacuolar routes in tobacco epidermal cells," Plant J., vol. 76, no. 1, 2013. DOI: 10.1111/tpj.12274
9. De Caroli M., Lenucci M. S., Di Sansebastiano G.-P., Dalessandro G., De Lorenzo G. and Piro G., "Protein trafficking to the cell wall occurs through mechanisms distinguishable from default sorting in tobacco," Plant J., vol. 65, no. 2, pp. 295–308, Jan. 2011. DOI: 10.1111/j.1365-313X.2010.04421.x
10. Di Sansebastiano G.-P., Barozzi, F., Piro, G., Denecke, J., Lousa, C. De M., "Trafficking routes to the plant vacuole: connecting alternative and classical pathways." J. Exp Botany, vol. 69, no. 1, pp. 79-90, 2017. DOI: 10.1093/jxb/erx376
11. De Marchis F., Bellucci M., and Pompa A., "Unconventional pathways of secretory plant proteins from the endoplasmic reticulum to the vacuole bypassing the Golgi complex.," Plant Signal. Behav., vol. 8, no. 8, Aug. 2013. DOI: 10.4161/psb.25129
12. Pereira C., Soares da Costa, D., Pereira, S., de Moura Nogueira, F., Albuquerque, P. M., Teixeira, J., Faro, C. and Pissarra, J. "Cardosins in postembryonic development of cardoon: towards an elucidation of the biological function of plant aspartic proteinases," Protoplasma, vol. 232, no. 3–4, pp. 203–213, Apr. 2008. DOI: 10.1007/s00709-008-0288-9
13. Okamoto T., "Transport of Proteases to the Vacuole: ER Export Bypassing Golgi ?," Plant Cell, no. February, 2006. DOI: 10.1007/7089
14. Egas, C., Lavoura, N., Resende, R., Brito, R. M. M., Pires, E., de Lima, M. C. P. and Faro, C., "The Saposin-like Domain of the Plant Aspartic Proteinase Precursor Is a Potent Inducer of Vesicle Leakage," J. Biol. Chem., vol. 275, no. 49, pp. 38190–38196, Dec. 2002. DOI: 10.1074/jbc.m006093200
15. Dupuis J. H., Hua Y., Habibi, M., Peng, X., Plotkin, S. S., Wang, S., Song, C. and Yada, R. Y. "pH dependent membrane binding of the Solanum tuberosum plant specific insert: An in silico study," Biochim. Biophys. Acta - Biomembr., vol. 1860, no. 12, pp. 2608–2618, Dec. 2018. DOI: 10.1016/j.bbamem.2018.10.001
16. De Moura D. C., Bryksa B. C. and Yada R. Y., "In silico insights into protein-protein interactions and folding dynamics of the saposin-like domain of Solanum tuberosum aspartic protease," PLoS One, vol. 9, no. 9, pp. 18–22, 2014. DOI: 10.1371/journal.pone.0104315
17. Muñoz F. F., Mendieta J. R., Pagano M. R., Paggi R. A., Daleo G. R. and Guevara M. G., "The swaposin-like domain of potato aspartic protease (StAsp-PSI) exerts antimicrobial activity on plant and human pathogens," Peptides, vol. 31, no. 5, pp. 777–785, 2010. DOI: 10.1016/j.peptides.2010.02.001
18. Curto P., Lufrano, D., Pinto, C., Custódio, V., Gomes, A., Bakás, L., Vairo-Cavalli, S., Faro, C. and Simões, I., "Establishing the yeast kluyveromyces lactis as an expression host for production of the saposin-like domain of the aspartic protease cirsin," Appl. Environ. Microbiol., vol. 80, no. 1, pp. 86–96, 2014. DOI: 10.1128/AEM.03151-13
19. Terauchi K., Asakura, T., Ueda, H., Tamura, T., Tamura, K., Matsumoto, I., Misaka, T., Hara-Nishimura, I. and Abe, K., "Plant-specific insertions in the soybean aspartic proteinases, soyAP1 and soyAP2, perform different functions of vacuolar targeting.," J. Plant Physiol., vol. 163, no. 8, pp. 856–62, Jul. 2006. DOI: 10.1016/j.jplph.2005.08.007
20. Frey M. E., D'Ippolito S., Pepe A., Daleo G. R., and Guevara M. G., "Transgenic expression of plant-specific insert of potato aspartic proteases (StAP-PSI) confers enhanced resistance to Botrytis cinerea in Arabidopsis thaliana," Phytochemistry, vol. 149, pp. 1–11, May 2018. DOI: 10.1016/j.phytochem.2018.02.004
21. Törmäkangas K., Hadlington, J. L., Pimpl, P., Hillmer, S., Brandizzi, F., Teeri, T. H. and Denecke, J., "A Vacuolar Sorting Domain May Also Influence the Way in Which Proteins Leave the Endoplasmic Reticulum," Plant Cell, vol. 13, no. 9, p. 2021, Sep. 2007. DOI: 10.2307/3871425
22. Boevink P., Oparka K., Cruz S. S., Martin B., Betteridge A. and Hawes C., "Stacks on tracks: the plant Golgi apparatus traffics on an actin/ER network," Plant J., vol. 15, no. 3, pp. 441–447, Aug. 1998. DOI: 10.1046/j.1365-313X.1998.00208.x
23. Saint-Jore C. M., Evins J., Batoko H., Brandizzi F., Moore I. and Hawes C., "Redistribution of membrane proteins between the Golgi apparatus and endoplasmic reticulum in plants is reversible and not dependent on cytoskeletal networks," Plant J., vol. 29, no. 5, pp. 661–678, Mar. 2002. DOI: 10.1046/j.0960-7412.2002.01252.x

24. daSilva, L.P., Snapp, E. L., Denecke, J., Lippincott-Schwartz, J., Hawes, C. and Brandizzi, F., "Endoplasmic Reticulum Export Sites and Golgi Bodies Behave as Single Mobile Secretory Units in Plant Cells", Plant Cell, vol. 16, no. 7, pp. 1753-1771, 2004. DOI: 10.1105/tpc.022673
25. Osterrieder, A., Hummel, E., Carvalho, C. M. and Hawes, C. "Golgi membrane dynamics after induction of a dominant-negative mutant Sar1 GTPase in tobacco", J. Exp. Bot., vol. 61, no. 2, pp. 405-422, 2010. DOI: 10.1093/jxb/erp315
26. Satiat-Jeunemaitre B. and Hawes C., "Redistribution of a Golgi glycoprotein in plant cells treated with Brefeldin A," J. Cell Sci., vol. 103, no. 4, pp. 1153–1166, Dec. 1992.
27. Hanton S. L., Renna L., Bortolotti L. E., Chatre L., Stefano G. and Brandizzi F., "Diacidic Motifs Influence the Export of Transmembrane Proteins from the Endoplasmic Reticulum in Plant Cells." The Plant Cell, vol. 17, pp. 3081-3093, 2005. DOI: 10.1105/tpc.105.034900
28. Osterrieder, A., Carvalho, C. M., Latijnhouwers, M., Johansen, J. N., Stubbs, C., Botchway, S. and Hawes, C., "Fluorescence Lifetime Imaging of Interactions between Golgi Tethering Factors and Small GTPases in Plants", Traffic, vol. 10, no. 8, pp. 1034-1046, 2009. DOI: 10.1111/j.1600-0854.2009.00930.x
29. Batoko H., Zheng H. Q., Hawes C. and Moore I., "A rab1 GTPase is required for transport between the endoplasmic reticulum and Golgi apparatus and for normal Golgi movement in plants.," Plant Cell, vol. 12, no. 11, pp. 2201–18, Nov. 2000. DOI: 10.1105/tpc.12.11.2201
30. Kotzer A. M., Brandizzi F., Neumann U., Paris N., Moore I. and Hawes C., "AtRabF2b (Ara7) acts on the vacuolar trafficking pathway in tobacco leaf epidermal cells.," J. Cell Sci., vol. 117, no. Pt 26, pp. 6377–89, Dec. 2004. DOI: 10.1242/jcs.01564
31. Terauchi K., Nishizawa N. K., Matsumoto I., Abe K. and Asakura T., "Characterization of the genes for two soybean aspartic proteinases and analysis of their different tissue-dependent expression," Planta, vol. 218, no. 6, pp. 947–957, Apr. 2004. DOI: 10.1007/s00425-003-1179-0
32. Ramalho-Santos M., Veríssimo, P., Cortes, L., Samyn, B., Van Beeumen, J., Pires, E. and Faro, C., "Identification and proteolytic processing of procardosin A.," Eur. J. Biochem., vol. 255, no. 1, pp. 133–8, Jul. 1998. DOI: 10.1046/j.1432-1327.1998.2550133.x
33. Vieira M., Pissarra, J., Veríssimo, P., Castanheira, P., Costa, Y., Pires, E. and Faro, C., "Molecular cloning and characterization of cDNA encoding cardosin B, an aspartic proteinase accumulating extracellularly in the transmitting tissue of Cynara cardunculus L.," Plant Mol. Biol., vol. 45, no. 5, pp. 529–39, Mar. 2001.
34. Duarte P., Pissarra J., and Moore I., "Processing and trafficking of a single isoform of the aspartic proteinase cardosin A on the vacuolar pathway," Planta, vol. 227, no. 6, pp. 1255–1268, May 2008. DOI: 10.1007/s00425-008-0697-1
35. Costa D. S., Pereira S., Moore I., and Pissarra J., "Dissecting cardosin B trafficking pathways in heterologous systems," Planta, vol. 232, no. 6, pp. 1517–1530, Nov. 2010. DOI: 10.1007/s00425-010-1276-9
36. Oliveira A., Pereira, C., Soares da Costa, D., Teixeira, J., Fidalgo, F., Pereira, S. and Pissarra, J., "Characterization of aspartic proteinases in C. cardunculus L. callus tissue for its prospective transformation," Plant Sci., vol. 178, no. 2, pp. 140–146, 2010. DOI: 10.1016/j.plantsci.2009.11.008
37. Pissarra J., Pereira, C., Soares da Costa, D., Figueiredo, R., Duarte, P., Teixeira, J. and Pereira, S., "From Flower to Seed Germination in Cynara cardunculus: A Role for Aspartic Proteinases," Int. J. Plant Dev. Biol., pp. 274–281, 2007.
38. Soares A., Ribeiro Carlton, S. M. and Simões I., "Atypical and nucellin-like aspartic proteases: emerging players in plant developmental processes and stress responses," J. Exp. Bot., vol. 70, no. 7, pp. 2059–2076, Apr. 2019. DOI: 10.1093/jxb/erz034
39. Simões I. and Faro C., "Structure and function of plant aspartic proteinases.," Eur. J. Biochem., vol. 271, no. 11, pp. 2067–75, Jun. 2004. DOI: 10.1111/j.1432-1033.2004.04136.x
40. Muñoz F., Palomares-Jerez M. F., Daleo G., Villalaín J. and M. G. Guevara M. G., "Possible mechanism of structural transformations induced by StAsp-PSI in lipid membranes," Biochim. Biophys. Acta - Biomembr., vol. 1838, no. 1 PARTB, pp. 339–347, Jan. 2014. DOI: 10.1016/j.bbamem.2013.08.004
41. Paris N., Saint-Jean, B., Faraco, M., Krzeszowiec, W., Dalessandro, G., Neuhaus, J.-M., Di Sansebastiano, G. P. , "Expression of a glycosylated GFP as a bivalent reporter in exocytosis.," Plant Cell Rep., vol. 29, no. 1, pp. 79–86, Jan. 2010. DOI: 10.1007/s00299-009-0799-7
42. Rayon C., Lerouge P., and Faye L., "The protein N-glycosylation in plants," J. Exp. Bot., vol. 49, no. 326, pp. 1463–1472, 1998. DOI: 10.1093/jxb/49.326.1463
43. Wilkins T. A., Bednarek S. Y. and Raikhel N. V., "Role of propeptide glycan in post-translational processing and transport of barley lectin to vacuoles in transgenic tobacco.," Plant Cell, vol. 2, no. 4, pp. 301–13, Apr. 1990. DOI: 10.1105/tpc.2.4.301

687 44. Ramis C., Gomord V., Lerouge P., and Faye L., "Deglycosylation is necessary but not sufficient for
688 activation of proconcanavalin A," J. Exp. Bot., vol. 52, no. 358, pp. 911–917, May 2001. DOI:
689 10.1093/jexbot/52.358.911
690 45. Vitale A. and Raikhel N. V., "What do proteins need to reach different vacuoles?," Trends Plant Sci.,
691 vol. 4, no. 4, pp. 149–155, 1999. DOI: 10.1016/S1360-1385(99)01389-8
692 46. Occhialini A., Gouzerh G., Di Sansebastiano G. P. and Neuhaus J. M., "Dimerization of the vacuolar
693 receptors AtRMR1 and -2 from Arabidopsis thaliana contributes to their localization in the trans-Golgi
694 network," Int. J. Mol. Sci., vol. 17, no. 10, 2016. DOI: 10.3390/ijms17101661
695 47. Pompa A., De Marchis, F., Pallotta, M. T., Benitez-Alfonso, Y., Jones, A., Schipper, K., Moreau, K.,
696 Žárský, V., Di Sansebastiano, G. P. and Bellucci, M. "Unconventional transport routes of soluble and
697 membrane proteins and their role in developmental biology," Int. J. Mol. Sci., vol. 18, no. 4, 2017. DOI:
698 10.3390/ijms18040703
699 48. Goring D. R. and Di Sansebastiano G. P., "Protein and membrane trafficking routes in plants:
700 Conventional or unconventional?," J. Exp. Bot., vol. 69, no. 1, pp. 1–5, 2017. DOI: 10.1093/jxb/erx435
701 49. Kervinen J., Tobin G. J., Costa J., Waugh D. S., Wlodawer A. and Zdanov A., "Crystal structure of plant
702 aspartic proteinase prophytepsin: inactivation and vacuolar targeting.," EMBO J., vol. 18, no. 14, pp.
703 3947–55, Jul. 1999. DOI: 10.1093/emboj/18.14.3947
704 50. Sparkes I. A., Runions J., Kearns A. and Hawes C., "Rapid, transient expression of fluorescent
705 fusion proteins in tobacco plants and generation of stably transformed plants.," Nat. Protoc., vol. 1, no.
706 4, pp. 2019–25, Jan. 2006. DOI: 10.1038/nprot.2006.286
707 51. Curtis M. D. and Grossniklaus U., "Breakthrough Technologies A gateway Cloning Vector Set for
708 High-Throughput Functional Analysis of Genes in Planta," Plant Physiol. Vol. 133, pp. 462-469, 2003.
709 DOI: 10.1104/pp.103.027979